January 23, 2008

Optical Solitons in PT Periodic Potentials

Z. H. Musslimani, *Florida State University*
Konstantinos G. Makris, *University of Central Florida*
Ramy El-Ganainy, *University of Central Florida*
Demetrios N. Christodoulides, *University of Central Florida*

Optical Solitons in $\mathcal{PT}$ Periodic Potentials

Z. H. Musslimani

Department of Mathematics, Florida State University, Tallahassee, Florida 32306-4510, USA

K. G. Makris, R. El-Ganainy, and D. N. Christodoulides

College of Optics & Photonics-CREOL, University of Central Florida, Orlando, Florida 32816, USA

We investigate the effect of nonlinearity on beam dynamics in parity-time ($\mathcal{PT}$) symmetric potentials. We show that a novel class of one- and two-dimensional nonlinear self-trapped modes can exist in optical $\mathcal{PT}$ synthetic lattices. These solitons are shown to be stable over a wide range of potential parameters. The transverse power flow within these complex solitons is also examined.

Quantum mechanics demands that every physical observable is associated with a real spectrum and thus must be Hermitian. In the case of the Hamiltonian operator, this physical axiom not only implies real eigenenergies but also guarantees conservation of probability [1]. Yet in recent years, a series of studies by Bender and co-orkers has demonstrated that even non-Hermitian Hamiltonians can exhibit entirely real spectra provided they respect parity-time ($\mathcal{PT}$) symmetry [2]. By definition, a Hamiltonian belongs to this latter class as long as it shares a common set of eigenfunctions with the $\hat{P}\hat{T}$ operator. In general the action of the parity operator $\hat{P}$ is defined by the relations $\hat{p} \rightarrow -\hat{p}, \hat{x} \rightarrow -\hat{x}$ ($\hat{p}, \hat{x}$ stand for momentum and position operators, respectively) whereas that of the time operator $\hat{T}$ by $\hat{p} \rightarrow -\hat{p}, \hat{x} \rightarrow \hat{x}, i \rightarrow -i$. Given the fact that the action of $\hat{T}$ leads to a time reversal, i.e., $\hat{T}\hat{H} = \hat{p}^2/2 + V^*(x)$, one finds that $\hat{P}\hat{T}\hat{H} = \hat{H}\hat{P}\hat{T} = \hat{p}^2/2 + V^*(-x) = \hat{H}$. From here we conclude that a Hamiltonian is $\mathcal{PT}$ symmetric when the following condition is satisfied $V(x) = V^*(-x)$. Therefore the real part of a $\mathcal{PT}$ complex potential must be an even function of position whereas the imaginary component should be odd. Among the most intriguing characteristics of such a pseudo-Hermitian Hamiltonian, is the existence of a critical threshold above which the system undergoes a sudden phase transition because of spontaneous $\mathcal{PT}$ symmetry breaking. In this regime the spectrum is no longer real but instead it becomes complex. The relevance of these recent mathematical developments in quantum field theories and other areas of physics, has also been addressed in a number of studies [2–7].

Optics can provide a fertile ground where $\mathcal{PT}$ related concepts can be realized and experimentally tested. In fact, this can be achieved through a judicious inclusion of gain or loss regions in guided wave geometries [8]. Given that the complex refractive index distribution in a structure is $n(x) = n_0(x) + n_R(x) + in_I(x)$, one can deduce that $n(x)$ plays the role of the optical potential (where x represents the normalized transverse coordinate). The parity-time condition implies that the index waveguiding profile $n_R(x)$ should be even in the transverse direction while the loss or gain term $n_I(x)$ must be odd. In fact, gain or loss levels of approximately ± 40 cm^{-1} at wavelengths of ≈ 1 μm, that are typically encountered in standard quantum well semiconductor lasers or semiconductor optical amplifiers [8], will be sufficient to observe $\mathcal{PT}$ behavior. The imaginary part of the $\mathcal{PT}$ potential in such SOA arrangements can alternate between gain and loss in a diatomic waveguide lattice configuration depending on whether the input current is used above or below lasing threshold. Of interest will be to synthesize periodic systems [9] that can exhibit novel features stemming from parity-time symmetry. Even more importantly, the involvement of optical nonlinearities (quadratic, cubic, photorefractive nonlinearities, etc.[10]), may allow the study of such configurations under nonlinear conditions.

In this Letter we show that $\mathcal{PT}$ symmetric nonlinear lattices can support soliton solutions. These self-trapped states can be stable over a wide range of parameters in spite of the fact that gain or loss regions are present in this system. We first consider the propagation dynamics of nonlinear beams in a single $\mathcal{PT}$ waveguide cell and then we examine their behavior in a $\mathcal{PT}$ symmetric optical lattice. Both 1D and 2D soliton solutions are presented along with their associated transverse power-flow density. Our analysis sheds light for the first time on the interplay between nonlinearity and parity-time symmetry. Interestingly enough, even in the presence of relatively strong gain or loss effects, stationary self-trapped states (single cell and lattice) can exist with real propagation eigenvalues. This is a direct outcome of the $\mathcal{PT}$ symmetric nature of the potentials involved. It is important to stress that our results are fundamentally different from those previously obtained within the context of complex Ginzburg-Landau (GL) systems [11].

We begin our analysis by considering optical wave propagation in a self-focusing Kerr nonlinear $\mathcal{PT}$ symmetric potential. In this case, the beam evolution is governed by the following normalized nonlinear Schrödinger-

like equation,

$$i\frac{\partial \psi}{\partial z} + \frac{\partial^2 \psi}{\partial x^2} + [V(x) + iW(x)]\psi + |\psi|^2\psi = 0, \quad (1)$$

where ψ is proportional to the electric field envelope and z is a scaled propagation distance. Based on the previous discussion, the real and the imaginary components of the $\mathcal{PT}$ symmetric potential satisfy the following relations $V(-x) = V(x)$, $W(-x) = -W(x)$, respectively. Physically, $V(x)$ is associated with index guiding while $W(x)$ represents the gain or loss distribution of the optical potential. Note that in the linear regime, Eq. (1) conserves the "quasipower" $Q(z) = \int_{-\infty}^{+\infty} \psi(x, z)\psi^*(-x, z)dx$ as opposed to the actual electromagnetic power, $P(z) = \int_{-\infty}^{+\infty} |\psi(x, z)|^2 dx$ [12]. In the nonlinear domain however, these quantities evolve according to $i\frac{dQ}{dz} + \int_{-\infty}^{+\infty} \psi(x, z)\psi^*(-x, z)[|\psi(x, z)|^2 - |\psi(-x, z)|^2]dx = 0$ and $\frac{dP}{dz} + 2\int_{-\infty}^{+\infty} W(x)|\psi(x, z)|^2 dx = 0$.

Stationary soliton solutions to Eq. (1) are sought in the form $\psi(x, z) = \phi(x)\exp(i\lambda z)$ where $\phi(x)$ is the nonlinear eigenmode and λ is the corresponding real propagation constant. In this case ϕ satisfies

$$\frac{d^2\phi}{dx^2} + [V(x) + iW(x)]\phi + |\phi|^2\phi = \lambda\phi. \quad (2)$$

In order to determine the linear stability properties of such self-trapped localized modes, we consider small perturbations on the solutions of Eq. (1) of the form [13],

$$\psi(x, z) = \phi(x)e^{i\lambda z} + \varepsilon[F(x)e^{i\sigma z} + G^*(x)e^{-i\sigma^* z}]e^{i\lambda z}, \quad (3)$$

where $\varepsilon \ll 1$. Here, F and G are the perturbation eigenfunctions and σ indicates the growth rate of the perturbation. By linearizing Eq. (1) around the localized solution $\phi(x)$ we obtain the following linear eigenvalue problem for the perturbation modes

$$\begin{pmatrix} \hat{L} & \phi^2 \\ -\phi^{*2} & -\hat{L}^* \end{pmatrix}\begin{pmatrix} F \\ G \end{pmatrix} = \sigma\begin{pmatrix} F \\ G \end{pmatrix}, \quad (4)$$

where $\hat{L} = \frac{d^2}{dx^2} + V(x) + iW(x) + 2|\phi|^2 - \lambda$. Evidently, the $\mathcal{PT}$ nonlinear modes are linearly unstable if σ has an imaginary component, while they are stable if σ is real.

Before we consider light self-trapping in complex lattices, it is important to first understand nonlinear optical beam dynamics in a single $\mathcal{PT}$ complex potential. For illustration purposes, we assume a Scarff II potential, e.g.,

$$V(x) = V_0 \operatorname{sech}^2(x), \quad W(x) = W_0 \operatorname{sech}(x)\tanh(x), \quad (5)$$

with V_0 and W_0 being the amplitudes of the real and imaginary part. Notice that the corresponding linear problem associated with the potential of Eq. (5) exhibits an entirely real spectrum provided that, $W_0 \le V_0 + 1/4$ [14]. Thus for a fixed value of V_0, there exists a threshold for the imaginary amplitude W_0. Above this so-called $\mathcal{PT}$ threshold, a phase transition occurs and the spectrum enters the complex domain. Interestingly enough, even if the Scarff

potential of Eq. (5) has crossed the phase transition point (its spectrum is complex), nonlinear states can still be found with real eigenvalues. In other words, the beam itself can alter the amplitude of the refractive index distribution through the optical nonlinearity. Thus for a given W_0, this new effective potential nonlinearly shifts the $\mathcal{PT}$ V_0 threshold and in turn allows nonlinear eigenmodes with real eigenvalues to exist. In contrast, at lower power levels the parity-time symmetry cannot be nonlinearly restored and hence remains broken. A nonlinear mode of this potential corresponding to $\lambda = 0.98$, when $V_0 = 1$, $W_0 = 0.5$ is shown in Fig. 1. Equation (2) admits an exact solution of the form $\phi = \phi_0 \operatorname{sech}(x)\exp\{i\mu\tan^{-1}[\sinh(x)]\}$, where $\mu = W_0/3$, $\lambda = 1$ and $\phi_0 = \sqrt{2 - V_0 + (W_0^2/9)}$. We next examine the stability of these nonlinear modes by numerically solving the corresponding perturbation eigenvalue problem of Eq. (4). To support the linear stability results we have checked the robustness of each nonlinear state using beam propagation methods and by adding random noise on both amplitude and phase. The results of this simulation, shown in Fig. 1 for $V_0 = 1$, $W_0 = 0.5$, indicate that the beam is nonlinearly stable. To shed more light on the properties of these nonlinear solutions, we examine the quantity $S = (i/2)(\phi \phi_x^* - \phi^* \phi_x)$ associated with the transverse power-flow density or Poynting vector across the beam. This energy flow arises from the nontrivial phase structure of these nonlinear modes. For the analytical solution mentioned above we find that $S = (W_0\phi_0^2/3)\operatorname{sech}^3(x)$. Obviously, S is everywhere positive in this $\mathcal{PT}$ cell, thus implying that the power always flows in one direction, i.e., from the gain toward the loss region.

We next investigate optical solitons and their dynamics in nonlinear periodic $\mathcal{PT}$ potentials. Since the general idea holds for any such complex potential, we here consider for simplicity the case

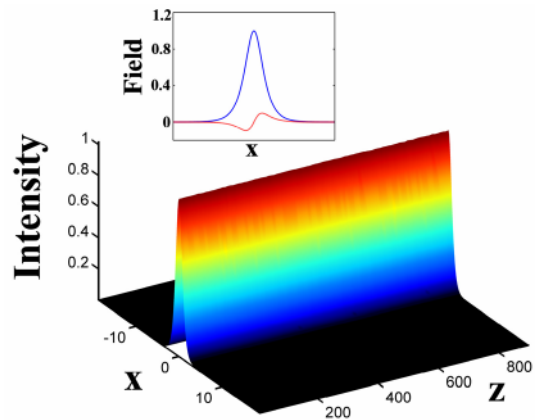$$V(x) = \cos^2(x), \quad W(x) = W_0 \sin(2x). \quad (6)$$

FIG. 1 (color online). Intensity evolution of a nonlinear mode in a $\mathcal{PT}$ Scarff II potential, when $\lambda = 0.98$. The inset depicts the real (solid blue curve) and imaginary (dotted red curve) component of such an eigenmode.

The linear properties of such a periodic potential can be understood by examining the corresponding linear problem of Eq. (2), i.e., $\frac{d^2\phi}{dx^2} + [V(x) + iW(x)]\phi = \lambda\phi$, where λ now represents the propagation constant in the periodic structure. Since the potentials $V(x)$, $W(x)$ of Eq. (6) are π-periodic, the Floquet-Bloch theorem dictates that the eigenfunctions are of the form $\phi = \Phi_k(x)\exp(ikx)$, where $\Phi_k(x + \pi) = \Phi_k(x)$ and k stands for the real Bloch momentum. We note that in general the band structure of a complex lattice can be complex. Yet, for periodic $\mathcal{PT}$ symmetric potentials, the band diagram can be entirely real as long as the system is operated below the phase transition point (unbroken $\mathcal{PT}$ symmetry). For the particular potential of Eq. (6), we find that purely real bands are possible in the range $0 \leq W_0 < 1/2$. In Fig. 2 we show the associated band structure for various values of the potential parameter W_0 (below and above the phase transition point $W_0 = 1/2$). We notice that as W_0 is increased the band gap becomes narrower and closes completely when crossing the critical transition value $W_0 = 1/2$. Pseudo-Hermitian periodic potentials having zero $\mathcal{PT}$ threshold were also discussed [15].

Having found the band-gap structure, we next obtain soliton solutions to Eq. (2) when the complex potential is given by Eq. (6). For $W_0 < 1/2$, we numerically construct a family of localized solutions with real eigenvalues located within the semi-infinite "energy" gap. A typical field profile of such a soliton is shown in Fig. 3(a). We next address the stability of these solutions given that these complex structures involve strong loss and gain. In general we found that the instability growth rate tends to increase with W_0. In addition, narrower self-trapped waves are more stable since the nonlinearity tends to further enhance the index guiding, thus perturbing the local $\mathcal{PT}$ phase transition point. To further examine the robustness of these $\mathcal{PT}$ lattice self-trapped modes, beam propagation methods were used. Under linear conditions symmetric diffraction occurs in this periodic complex system. On the other hand, as the power is increased the beam becomes confined
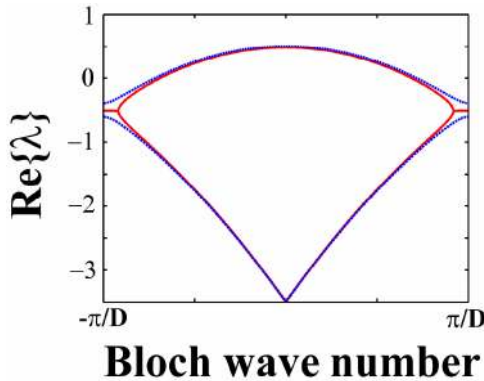
and propagates undistorted, thus forming a lattice soliton in spite of any symmetry breaking perturbations. Figure 3(b), shows the propagation dynamics of such a soliton (for $V_0 = 1$, $W_0 = 0.45$, $\lambda = 1.57$) as a function of the propagation distance. The transverse power flow is also plotted in Fig. 3(c). Unlike the single-cell case considered before, the power flow in this case is more involved. As indicated in Fig. 3(c), the direction of the flow from gain to loss regions varies across the lattice. More specifically, it is positive (from left to right) in the waveguides and becomes negative (from right to left) in the space between channels. This should be physically anticipated since power transport occurs always from gain to loss domains. We would like to emphasize that the distribution of the power-flow density in these self-trapped $\mathcal{PT}$ states differs from that encountered in Ginzburg-Landau dissipative solitons [11]. More specifically, in GL systems the power flow is an antisymmetric function of position whereas in $\mathcal{PT}$ lattices is even, as clearly indicated in Fig. 3(c).

Notice that it is also possible to find stationary self-trapped modes with real propagation eigenvalues even above the symmetry breaking point $W_0 = 1/2$, as shown in the inset of Fig. 4. This is due to the fact that part of the band structure still remains real even above the $\mathcal{PT}$ threshold [Fig. 2]. This family of solitons exists provided that the Fourier spectrum of these solutions (in Bloch-momentum space) is primarily contained within the region where the band is real (λ *real*) located around the $k = 0$ point. Stability analysis however reveals that this latter class of lattice solitons is in fact unstable. This instability is corroborated by numerical simulations, as shown in Fig. 4.

Finally, we discuss the formation of $\mathcal{PT}$ lattice solitons in two-dimensional periodic geometries. In this case, Eq. (1) becomes $i\frac{\partial\psi}{\partial z} + \nabla^2\psi + [V + iW]\psi + |\psi|^2\psi = 0$,
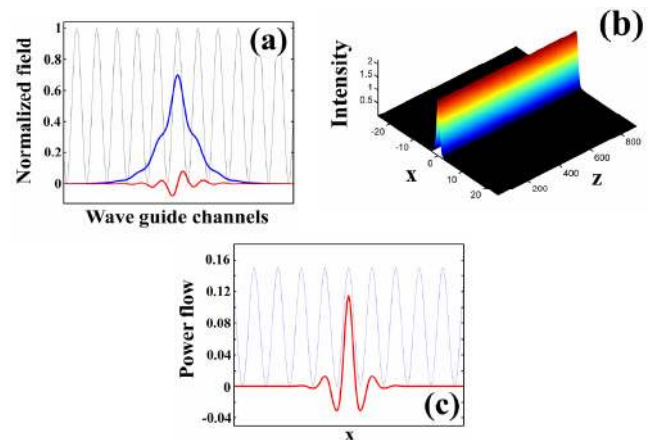
FIG. 3 (color online).   (a) $\mathcal{PT}$ lattice ($W_0 = 0.45$) soliton field profile (real part: blue line, imaginary part: red line) for $\lambda = 0.7$. (b) Stable propagation of a $\mathcal{PT}$ lattice soliton with eigenvalue $\lambda = 1.57$. (c) Transverse power flow (solid line) of the soliton in (a) across the lattice. The dotted line represents the real part of the potential in both (a) and (c).
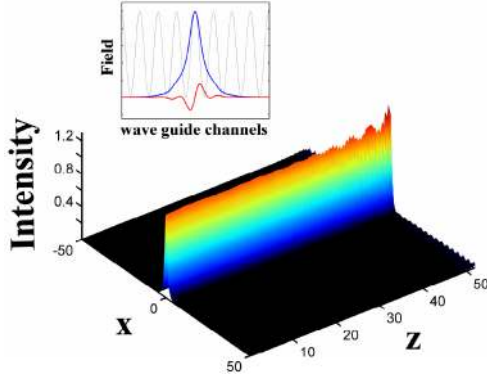
FIG. 2 (color online).   (a) Bandstructure for the $\mathcal{PT}$ potential $V(x) = \cos^2(x) + iW_0\sin(2x)$, when $W_0 = 0.45$ (dotted line), and $W_0 = 0.6$ (solid line).

FIG. 4 (color online). Intensity evolution of an unstable $\mathcal{PT}$ soliton above the phase transition point ($W_0 = 0.6$). The inset depicts the field profile (real part/blue line, imaginary part/red line) of an unstable $\mathcal{PT}$ soliton.

where again the potentials V and W obey the $\mathcal{PT}$ symmetry requirement, $V(-x, -y) = V(x, y)$ and $W(-x, -y) = -W(x, y)$. In Fig. 5(a) the band structure corresponding to the periodic potentials $V(x, y) = \cos^2(x) + \cos^2(y)$ and $W(x, y) = W_0[\sin(2x) + \sin(2y)]$ is depicted for $W_0 = 0.3$. It is instructive to observe that the symmetry breaking level for this two-dimensional potential is identical to the one-dimensional case ($W_0 = 0.5$). Above this phase transition point the first two bands merge together forming an oval, a double-valued surface (upon which all the propagation constants are real) attached to a 2D membrane of complex eigenvalues. A two-dimensional $\mathcal{PT}$ symmetric
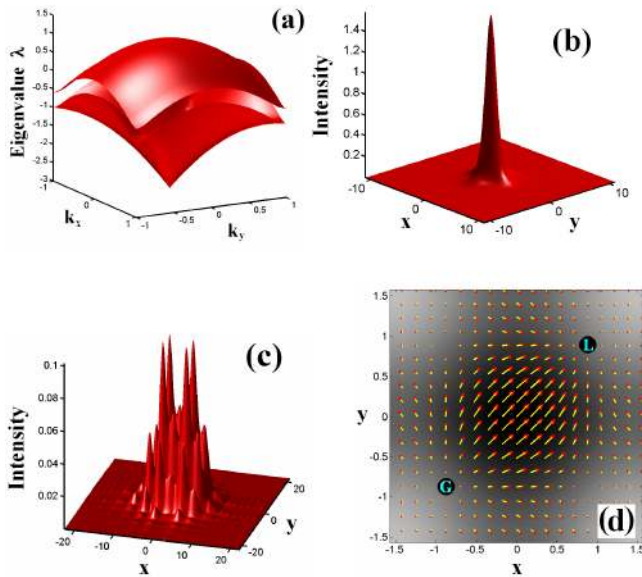
soliton with eigenvalues within the semi-infinite gap is shown in Fig. 5(b). At low intensities, the nonlinearity is not strong enough and hence this beam asymmetrically diffracts in this complex lattice as shown in Fig. 5(c). At soliton power levels, however, this nonlinear wave propagates in a stable fashion. To further understand the internal structure of these self-trapped states, we plot the transverse power-flow vector (Poynting vector) $\vec{S} = (i/2)[\phi \, \nabla\phi^* - \phi^* \nabla\phi]$, as shown in Fig. 5(d), which indicates again energy exchange among gain or loss domains.

In conclusion, a new class of one- and two-dimensional nonlinear self-trapped modes residing in parity-time symmetric wells and lattices is reported. The existence, stability, and propagation dynamics of such $\mathcal{PT}$ solitons were examined in detail.

FIG. 5 (color online).   (a) Band structure of a 2D-$\mathcal{PT}$ potential when $W_0 = 0.3$. (b) The intensity profile of a $\mathcal{PT}$ soliton when the propagation eigenvalues is $\lambda = 1.3$. (c) Linear diffraction pattern under single channel excitation (soliton input with $\lambda = 1.3$), and (d) Transverse power flow of this $\mathcal{PT}$ soliton solution within one cell where the dark area of the background represents the waveguide area. The regions where the gain or loss is maximum are indicated by the G, L points, respectively.

[1] A. Messiah, *Quantum Mechanics* (Dover, New York, 1999).
[2] C. M. Bender and S. Boettcher, Phys. Rev. Lett. **80**, 5243 (1998).
[3] C. M. Bender, D. C. Brody, and H. F. Jones, Phys. Rev. Lett. **89**, 270401 (2002); C. M. Bender, Am. J. Phys. **71**, 1095 (2003); Z. Ahmed, Phys. Lett. A **282**, 343 (2001).
[4] C. M. Bender *et al.*, Phys. Rev. Lett. **98**, 040403 (2007).
[5] M. Znojil, Phys. Lett. A **285**, 7 (2001); C. M. Bender *et al.*, J. Phys. A **40**, F153 (2007); G. Levai, J. Phys. A **40**, F273 (2007).
[6] I. Y. Goldsheid and B. A. Khoruzhenko, Phys. Rev. Lett. **80**, 2897 (1998); B. Bagchi and C. Quesne, Phys. Lett. A **273**, 285 (2000); H. Markum, R. Pullirsch, and T. Wettig, Phys. Rev. Lett. **83**, 484 (1999).
[7] M. V. Berry and H. J. O'Dell, J. Phys. A **31**, 2093 (1998); M. V. Berry, J. Phys. A **31**, 3493 (1998); D. O. Chudesnikov and V. P. Yakovlev, Laser Phys. **1**, 111 (1991); C. Keller *et al.*, Phys. Rev. Lett. **79**, 3327 (1997).
[8] A. E. Siegman, *Lasers* (University Science Books, Sausalito, CA, 1986); E. A. Ultanir, G. I. Stegeman, and D. N. Christodoulides, Opt. Lett. **29**, 845 (2004).
[9] D. N. Christodoulides, F. Lederer, and Y. Silberberg, Nature (London) **424**, 817 (2003).
[10] S. Trillo and W. Torruellas, *Spatial Solitons* (Springer, New York, 2001).
[11] M. C. Cross and P. C. Hohenberg, Rev. Mod. Phys. **65**, 851 (1993); E. A. Ultanir, G. I. Stegeman, D. Michaelis, C. H. Lange, and F. Lederer, Phys. Rev. Lett. **90**, 253903 (2003); N. K. Efremidis and D. N. Christodoulides, Phys. Rev. E **67**, 026606 (2003); N. Akhmediev and A. A. Ankiewicz, *Dissipative Solitons* (Springer, New York, 2005).
[12] B. Bagchi, C. Quesne, and M. Znojil, Mod. Phys. Lett. A **16**, 2047 (2001).
[13] E. A. Kuznetsov, A. M. Rubenchik, and V. E. Zakharov, Phys. Rep. **142**, 103 (1986).
[14] Z. Ahmed, Phys. Lett. A **282**, 343 (2001).
[15] C. M. Bender, G. V. Dunne, and P. N. Meisinger, Phys. Lett. A **252**, 272 (1999); H. F. Jones, Phys. Lett. A **262**, 242 (1999); J. K. Boyd, J. Math. Phys. (N.Y.) **42**, 15 (2001); E. Narevicius, P. Serra, and N. Moiseyev, Europhys. Lett. **62**, 789 (2003).